Materials Advances

ROYAL SOCIETY OF CHEMISTRY

PAPER

View Article Online
View Journal | View Issue

Cite this: *Mater. Adv.*, 2025, 6, 6868

Very high temperature annealing of Cu_2O obtained by the bifacial oxidation of free-standing Cu foils

Matthew Zervos,*[a] George M. Georgiadis,[a] Ioannis Paschos,[bc] Matin Ashurov[bc] and Pavlos Savvidis[bcd]

Received 13th June 2025,
Accepted 19th August 2025

DOI: 10.1039/d5ma00642b

rsc.li/materials-advances

Cu_2O has been obtained *via* the thermal oxidation of free-standing Cu foils with a thickness of 127 μm under Ar and O_2 at 1020 °C followed by controlled cooldown at −5 °C at low pressure under an inert flow of Ar. We obtain single crystal grains of Cu_2O with sizes of ∼500 × 500 μm^2 which have a cubic crystal structure, but these extend only halfway through the bulk down to a layer of Kirkendall voids due to the bifacial oxidation of the Cu. The voids are nearly eliminated by annealing between 1120 °C and 1160 °C under Ar which also leads to grain growth. However, the out diffusion of the voids through the single crystal Cu_2O grains is accompanied by the formation of holes at the surface. We show that the layer of voids can be removed by polishing the Cu_2O down to ∼10 μm in order to preserve the single crystal nature of the grains obtained at 1020 °C while keeping the thermal budget to a minimum and discuss the limitations in exploiting the Cu_2O obtained in this way for the fabrication of devices.

1. Introduction

Cu_2O is a p-type metal oxide semiconductor that has a cubic crystal structure and a direct energy band gap of 2.1 eV. It is an archetype for the study of excitons that were observed for the first time in Cu_2O by Gross *et al.*[1] It has also been suggested to be suitable as a solar cell absorber given that it has a high absorption coefficient of $\alpha \sim 10^5$ in the visible[2] but so far solar cell device efficiencies have been limited to less than 10%.[3] In addition, Cu_2O has been shown to have very good photocatalytic properties for water splitting[4] but also for CO_2 reduction.[5]

Consequently, Cu_2O is still an active topic of ongoing investigation that attracted even more attention after the observation of giant Rydberg excitons with principal quantum numbers up to n = 25 by Kazimierczuk *et al.*[6] which in turn instigated further interest into the possibility of adding long-range interactions to the physics of exciton–polaritons that were recently detected in a $SiO_2/Ta_2O_5/Cu_2O/Ta_2O_5/SiO_2$ Fabry–Pérot cavity by Orfanakis *et al.*[7] Giant Rydberg excitons are attractive as solid-state counterparts of Rydberg atoms that are used in quantum computers, but so far, giant Rydberg excitons with $n > 10$ and polaritons have only been observed in naturally occurring crystals of Cu_2O. It is necessary then to grow high crystal quality Cu_2O on par with that occurring in nature.

In the past, Cu_2O has been obtained by many different methods such as molecular beam epitaxy (MBE),[8] atomic layer deposition (ALD)[9] pulsed laser deposition (PLD)[10] electrodeposition (ELD)[11] aerosol assisted chemical vapor deposition (AACVD)[12] successive ionic layer adsorption-reaction (SILAR)[13] and *e*-beam evaporation (EB)[14] but the crystal quality and phase purity of the Cu_2O obtained using most of the methods listed above is not comparable to that of naturally occurring single crystals. Only Steinhauer *et al.*[14] observed Rydberg excitons up to n = 6 in Cu_2O crystals obtained by thermal oxidation of 700 nm Cu deposited by *e*-beam evaporation (EB) on Si. Rydberg excitons with higher principal quantum numbers up to n = 10 have only been observed in (a) free standing Cu_2O prepared by thermal oxidation of Cu foils and (b) Cu_2O ingots grown by the optical float zone method using Cu_2O feed and seed rods obtained by thermal oxidation of 3–7 mm diameter Cu rods.

Early efforts in obtaining single crystal Cu_2O by thermal oxidation of Cu date back to the 1950's[15–18] but these were not always successful and polycrystalline Cu_2O with small grains were obtained. Interestingly, high crystal quality Cu_2O was successfully and consistently obtained in the 1960's by Toth *et al.*[19] *via* the high temperature oxidation of Cu foils in air between 1020 °C and 1040 °C followed by annealing at higher

[a] *Nanostructured Materials and Devices Laboratory, School of Engineering, University of Cyprus, PO Box 20537, Nicosia, 1678, Cyprus. E-mail: matthew.zervos@ucy.ac.cy*
[b] *Department of Physics, School of Science, Westlake University, Hangzhou 310014, China*
[c] *Institute of Natural Sciences, Westlake Institute for Advanced Study, Hangzhou, Zhejiang 310024, China*
[d] *Department of Materials Science and Engineering, University of Crete, P.O. Box 2208, 71003 Heraklion, Greece*

temperatures between 1085 °C and 1115 °C for times ranging between 5 and 150 h. The average annealing temperature for 0.76 mm thick Cu was 1085 °C while that used for 0.38 mm Cu was 1115 °C. The Cu_2O was retracted rapidly in less than 10 s at the end of annealing and the CuO that formed on top of the Cu_2O was removed in HNO_3 (aq) or by the use of abrasives. Large grains of 160 mm^2 were obtained from 0.203 mm and 0.254 mm thick Cu after oxidation at 1035 °C for 60 min and annealing at 1120 °C for 5 h. In contrast the Cu_2O obtained from 0.762 mm thick Cu had to be annealed for 100 h.[19]

After the breakthrough of Toth *et al.*[19] subsequent investigations focused mostly on the growth of single crystal ingots of Cu_2O by the optical, float zone method which allows one to cut wafers with a specific thickness that are flat. More specifically, Cu_2O was obtained in the 1970's by Brower *et al.*[20] *via* the floating zone method using Cu_2O feed rods prepared by thermal oxidation of Cu rods with diameters of 6.3 mm in air at 1050 °C for 96–100 h. A few years later Schmidt *et al.*[21] also obtained Cu_2O by the floating zone method that was subsequently annealed in air between 900 °C to 1050 °C. Many years later Chang *et al.*[22] prepared Cu_2O feed and seed rods *via* the thermal oxidation of high purity Cu rods with diameters between 4 and 7 mm that were oxidized in air for 3 days at 1045 °C. Cu_2O was grown by the optical float zone method and was cut into wafers with a thickness of ~1 mm and diameters of 7 mm after which they were annealed in air at 1045 °C for 1 to 4 days at one day intervals.[22] Similarly, Frazer *et al.*[23] prepared polycrystalline feed and seed rods of Cu_2O by thermal oxidation of copper metal rods at 1045 °C for 3 days. These were used to grow single crystal Cu_2O ingots by the floating zone method. Finally, Lynch *et al.*[24] prepared Cu_2O seed rods *via* the thermal oxidation of 5 mm Cu metal rods at 1100 °C for 40 hours in air that were used to grow single crystal Cu_2O by the optical float zone method and observed excitons with principal quantum numbers up to $n = 10$.

It should be emphasized at this point that all previous efforts into the growth of Cu_2O crystals *via* the optical float zone method were carried out using Cu_2O feed and seed rods prepared by the thermal oxidation of Cu rods in air up to temperatures of 1100 °C. The Cu rods had diameters up to 7 mm, so the Cu_2O ingots also had small diameters. The Cu_2O wafers were annealed between 1000 °C and 1050 °C and the time taken to obtain high crystal quality Cu_2O was of the order of many tens of hours *i.e.* days. It should also be noted that Cu_2O has not been grown by the Czochralski method due to the lack of suitable crucibles.

Besides all of the ongoing efforts into the growth of Cu_2O *via* the optical float zone method the thermal oxidation of Cu foils is also an active topic of ongoing investigation. For instance, Mani *et al.*[25] investigated the thermal oxidation of Cu (99.9%) foils with a thickness of ~0.12 mm at 1050 °C in air at atmospheric pressure for 1 h. The Cu_2O was annealed at 1130 °C for 15 h in air by increasing the temperature at a rate of 0.1 °C min^{-1}. After annealing the Cu_2O was cooled at 0.1 °C min^{-1} between plateaus of 1100, 1080, and 1050 °C, which were maintained for ~20 h each. For temperatures below 1050 °C, the pressure was adjusted to maintain the Cu_2O phase. Finally, at 700 °C the sample was quenched using a flow of cold Ar.[24] More recently Xiao *et al.*[26] showed that during oxidation of Cu the Cu_2O grains undergo rapid diffusion and move preferentially in the vertical growth direction to release the strain through the generation of Frank partial dislocations which grow by absorbing V_{Cu} and penetrate through the bulk. The Frank partial dislocations tend to slip along the lattice plane with the densest atoms, and the crystal rotates on the sliding surface, triggering grains to orient in a specific direction. Xiao *et al.*[26] showed that (111)-oriented Cu_2O with small grains are obtained by surface energy-dominated growth while the (110) oriented Cu_2O is obtained by strain-energy-driven grain growth.

Very recently we showed that high crystal quality and phase purity Cu_2O may be obtained in a controlled way *via* the thermal oxidation of Cu at 1020 °C under Ar and O_2 after annealing the Cu under H_2 which is very effective in reducing the bulk content of CuO in the Cu_2O.[27] After oxidation the Cu_2O was annealed for 60 min at 1040 °C resulting into ~500 × 500 μm^2 single crystal grains. The entire process lasted ~6 hours. The Cu_2O crystals obtained in this way consisted of (110) and (220) high index grains like those of Xiao *et al.*[26] but the Cu_2O crystal was retracted from the heated zone at 800 °C under a flow of Ar. The surface of the Cu_2O was covered by a semi-transparent layer of 10 nm CuO that acts as a natural passivation layer preventing the oxidation of the underlying Cu_2O upon exposure to air.[27] However, the single crystal grains of Cu_2O obtained in this way do not extend throughout the bulk due to the formation of a Kirkendall void layer (KVL) at the middle of the foil that was first identified but not directly observed by Toth *et al.* in the 1960's.[19] Recently Xiao *et al.*[26] observed this irregular KVL in Cu_2O by scanning electron microscopy (SEM). However, the Cu_2O of Xiao *et al.*[26] was derived by thermal oxidation of a 200 μm thick Cu foil at 1040 °C up to 3 h in air after which it was held at 1050 °C for 2 h under Ar but the Cu was in direct contact and constrained with corundum slides (Al_2O_3). The KVL must be removed as this will limit the lifetime of Rydberg excitons with large radii. Moreover, these voids are detrimental for devices *e.g.* p–n junction solar cells since there are allot of crystallographic imperfections in their vicinity with deep states residing in the energy gap of Cu_2O that will inevitably lead to the recombination of the photogenerated electron–hole pairs and which in turn will reduce the efficiency of solar cells.

Here we aim to obtain free standing Cu_2O with large single crystal, high purity grains *via* the oxidation of Cu foils in a time and cost-effective manner that can be used for the subsequent observation of Rydberg excitons. We show that annealing the Cu_2O above 1100 °C leads to grain growth and the elimination of the KVL but also to the formation of holes on the surface of the Cu_2O due to the out diffusion of the vacancies and voids. We argue that it is better to remove the KVL by polishing in order to preserve the single crystal nature of the Cu_2O grains residing above the KVL and keep the thermal budget to a minimum which in turn will make it feasible to isolate a single crystal grain for the purpose of optical spectroscopy. We also discuss the limitations in exploiting the Cu_2O obtained in this way for the fabrication of devices.

2. Methods

Cu foils with a thickness of 127 ± 4 μm and technical grade purity of 99.99% were cut and trimmed into rectangular pieces having different length to width ratios as shown in Fig. 1(a). All of the Cu foils had a width of 10 mm and were trimmed in such a way so that the grain direction due to rolling ran parallel to the long side. The length of the Cu foils was 20, 30 and 40 mm. Both sides of the Cu foil were polished to remove the ridges due to rolling after which they were flattened out between clean glass slides and their corners bent to form supports as shown in Fig. 1(b). Subsequently, the Cu was cleaned in isopropanol under ultrasonic vibration for 10 min in order to remove particles that got embedded into the Cu, dried with N_2 and annealed under a flow of Ar and H_2 in a 1″ hot wall, chemical vapor deposition (CVD) reactor capable of reaching 1200 °C, that was fed by a manifold consisting of four mass flow controllers connected to Ar, NH_3, O_2 and H_2. The reactor was initially purged with Ar and H_2 at room temperature for 10 min in order to remove traces of air after which the temperature was ramped up to 1000 °C at 30 °C min^{-1}. Upon reaching 1000 °C the same flow of Ar and H_2 was maintained for 180 min to reduce all oxides and promote grain growth. Cool-down was carried out under the same flow of Ar and H_2 all the way down to room temperature. A constant flow of 100 ml min^{-1} Ar and 100 ml min^{-1} H_2 at 10 mbar was maintained throughout the entire process. The Cu foils were removed at room temperature after purging with Ar and stored under vacuum in a desiccator with silica gel. The Cu foils with an overall length of 30 or 40 mm exhibited concave bending as shown in Fig. 1(c).

The Cu was converted into Cu_2O in a different 1″ hot wall reactor capable of reaching 1100 °C which was initially purged at room temperature for 10 min using a flow of 100 ml min^{-1} Ar and 100 ml min^{-1} H_2 to remove air after which the temperature was ramped up to 900 °C at 30 °C min^{-1} by maintaining the same flow of Ar and H_2 at 1 atm. At 900 °C the ramp rate was reduced to 10 °C min^{-1} until 1020 °C in order to prevent a temperature overshoot. Cu has a melting point of 1085 °C. At 1020 °C the same flow of Ar and H_2 was maintained for a further 30 min at 1 atm after which the flow of H_2 was interrupted and a flow of 100 ml min^{-1} Ar was maintained for 15 min in order to purge the H_2 and admit O_2. Subsequently the Cu foil was oxidized for 30 min under a flow of 100 ml min^{-1} Ar and 10 ml min^{-1} O_2. After oxidation the Cu_2O was cooled down in a controlled fashion at −5 °C min^{-1} under a flow of 100 Ar at 10^{-2} mbar all the way down to room temperature. A schematic illustration of the thermal oxidation of Cu at 1020 °C under Ar and O_2 is illustrated schematically in Fig. 2.

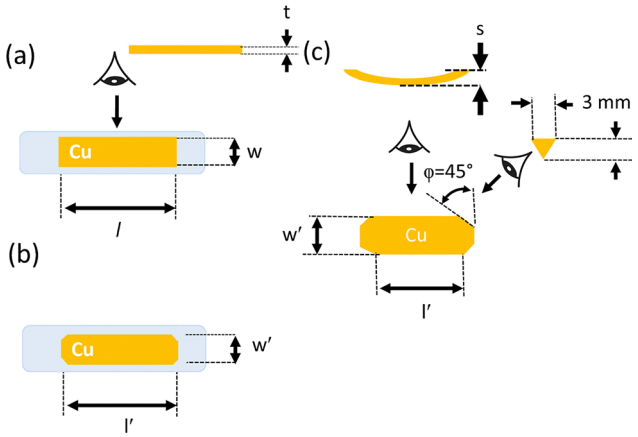

Fig. 1 Schematic diagram of (a) Cu foil with l = 20, 30 and 40 mm; w = 10 mm and t = 127 μm laid flat on a quartz boat (b) Cu with l' ∼ 16 mm; w' ∼ 6 mm and t = 127 μm standing on bent point corners (c) Cu with l' ∼ 36 mm; w' ∼ 6 mm and t = 127 μm showing the bending s = 3 mm that occurs after annealing under Ar and H_2 at 1000 °C.

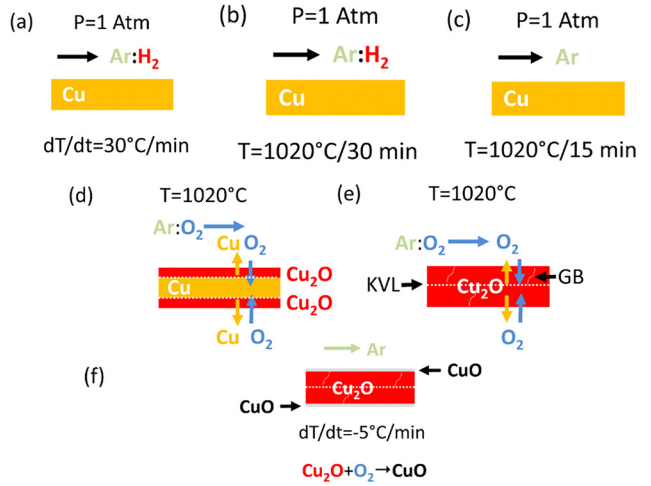

Fig. 2 Schematic representation of the process used for the growth of Cu_2O by thermal oxidation of Cu under Ar: O_2 (a) temperature ramp (b) short reduction and anneal of Cu under Ar: H_2 (c) purging of hydrogen (d) and (e) thermal oxidation and (f) controlled cool down.

Finally, the Cu_2O crystals obtained in this way were annealed in a different 1″ hot wall reactor capable of reaching 1500 °C, that was fed by a manifold also connected to Ar, O_2 and H_2. In this case the reactor was initially purged with 100 ml min^{-1} Ar at room temperature for 10 min in order to remove traces of air after which the temperature was ramped up to 1140 °C at 30 °C min^{-1} and 1 atm. Upon reaching 1140 °C the same flow of Ar was maintained for 1, 2, 3 and 4 hours at 1 atm. Cool-down was carried out under the same flow of Ar at −5 °C min^{-1} all the way down to room temperature. In addition, Cu_2O crystals were annealed at 1120, 1140 and 1160 °C for 60 min employing the same flows, ramp rate and cool down conditions.

The Cu_2O was inspected by optical transmission microscopy before and after annealing; the surface and section of the Cu_2O was also inspected by scanning electron microscopy (SEM) in order to identify the extent of the KVL while the crystal structure and phase purity was measured by X-ray diffraction (XRD) using a Rigaku Miniflex in the Bragg–Brentano θ–2θ geometry with a Cu K-a source and wavelength of 1.54Å at scan rate of 1° min^{-1}.

Finally, the KVL in the Cu_2O with no annealing was removed by polishing from the back side; this was achieved by using sapphire as a holder for the brittle Cu_2O crystal that was

covered by solid transparent wax. The wax on top of the Cu_2O was heated in a VT 6060P Thermo Scientific drying oven at 100 °C and 100 mbar in order to remove bubbles that formed during the melting of wax which upon cooling fixed the crystal in position. The Cu_2O was polished from the back side down to 10 μm using an Allied Opti Prep Precision Polishing System with ~0.5 μm diamond lapping surface. The structural properties of the Cu_2O obtained in this way were also investigated on section by SEM.

3. Results and discussion

We will begin by considering the preparation and properties of Cu which is important in obtaining high crystal quality and purity Cu_2O. A typical SEM image of a 127 μm thick Cu (99.99%) foil, as received, is shown in Fig. 3(a). The surface is not flat, and ridges run along the rolling direction that were removed by polishing as shown in Fig. 3(b). The Cu consists of small grains with sizes of 5 to 10 μm as shown in Fig. 3(c) and exhibited clear and well resolved peaks in the XRD corresponding to the (111), (200) and (311) crystallographic planes of the face centered cubic (fcc) crystal structure of Cu as shown in Fig. 4(a). We did not detect any peaks corresponding to CuO or Cu_2O. However, traces of oxides exist on the surface and inside the bulk Cu which must be eliminated in order to obtain high crystal quality and phase purity Cu_2O. Previous investigations have shown that a large flow of H_2 is very effective in reducing CuO and Cu_2O into metallic Cu. CuO is reduced to Cu_2O by H_2 at approximately 60 °C while complete reduction from Cu_2O to metallic Cu occurs at 480 °C.[28] Consequently, the Cu was annealed under Ar and H_2 at 1000 °C and 10 mbar for 3 hours to reduce all oxides and remove oxygen but also to promote grain growth. A typical SEM image of the 120 μm Cu foil after annealing is shown in Fig. 3(d) and (e). The Cu consists of grains as large as 200 μm and the surface is flattened to an extent due to the sublimation of Cu that occurs under the flow of Ar and H_2 at 10 mbar and 1000 °C which is lower than the melting point of Cu *i.e.* 1085 °C. The Cu exhibited clear peaks in the XRD after annealing as shown in Fig. 4(a) corresponding to the (111), (200) and (311) crystallographic planes of the fcc crystal structure of Cu. We find that annealing promotes the intensity of the peak corresponding to Cu grains with the (200) crystallographic orientation. The improvement in the crystal quality of the Cu is due to the fact that H_2 dissociates catalytically into H on the surface of Cu and penetrates into the Cu lattice promoting grain growth and eventually the formation of a single crystal. It has been shown that polycrystalline Cu, Ni,

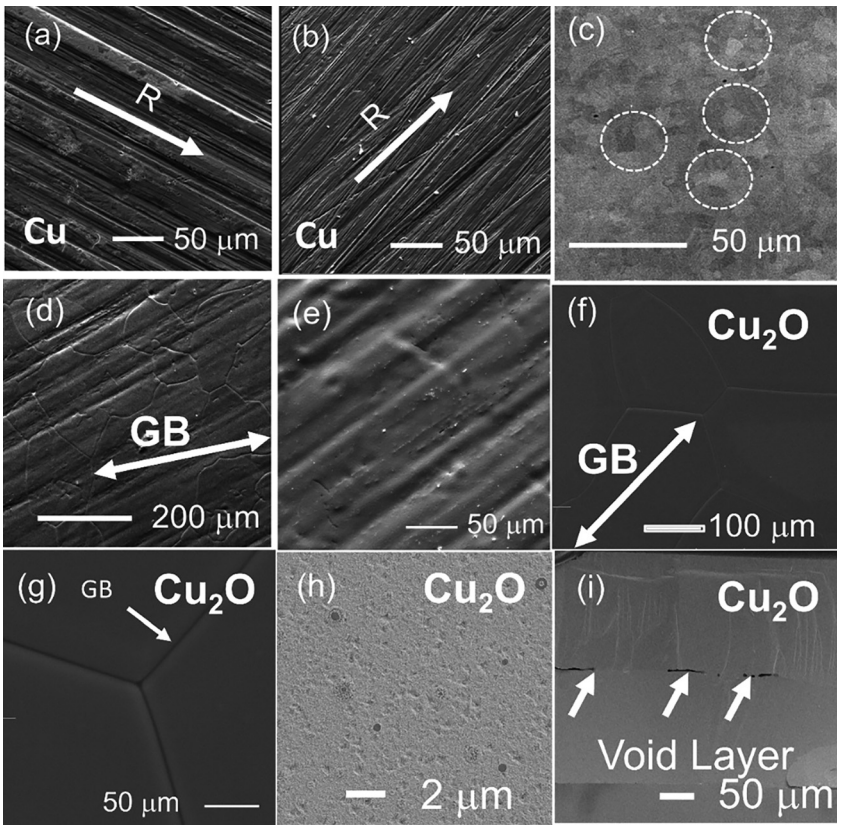

Fig. 3 SEM image of (a) Cu as-received showing the direction of rolling (b) Cu after polishing (c) Cu after fine polishing revealing grains with sizes up to 10 μm (d) and (e) Cu after annealing under Ar: H_2 at 1000 °C for 3 h showing the formation of grains with sizes >200 μm (f) Cu_2O after thermal oxidation at 1020 °C consisting of grains with sizes >200 μm (g) and (h) higher magnification images of Cu_2O showing that the surface is considerably flatter than that of Cu (i) section of Cu_2O showing the Kirkendall void layer at the middle extending over 50 μm at places.

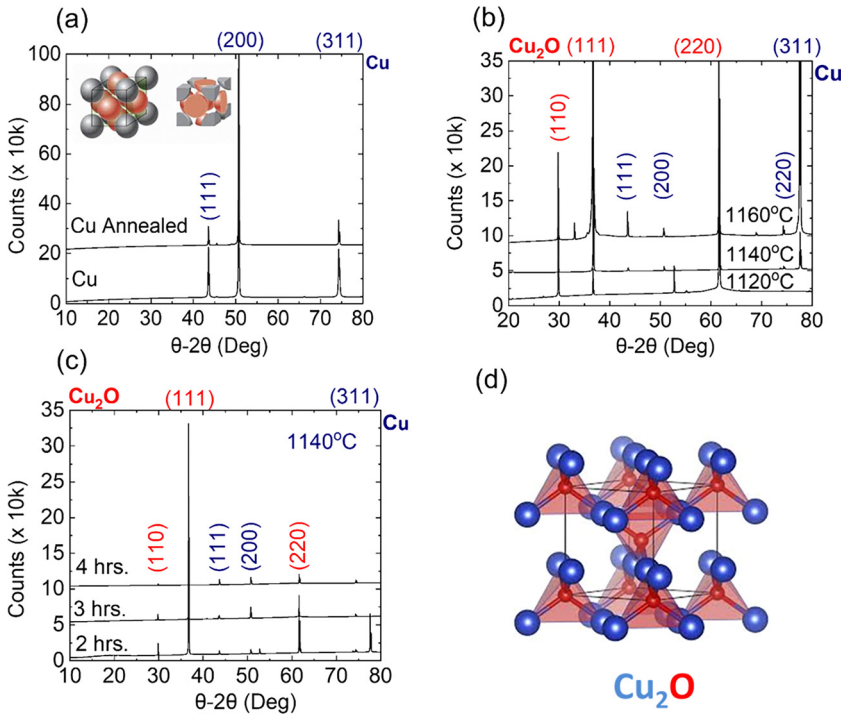

Fig. 4 XRD of (a) Cu as received and Cu after annealing under Ar: H_2 at 1000 °C for 3 h; inset shows the fcc crystal structure of Cu. (b) Cu_2O after annealing at 1120 °C, 1140 °C and 1160 °C for 3 h. (c) Cu_2O after annealing at 1140 °C, for 2, 3 and 4 h. (d) Crystal structure of Cu_2O.

and Co foils can't be converted into single crystals during annealing at high temperatures under Ar without H_2.[29] The Cu foils with lengths of 30 and 40 mm exhibited bending along their length as shown in Fig. 2(c). This is attributed to a reduction in the dislocation density and vacancies which in turn results in a crystal lattice with lower internal strain and an increase in ductility. This is not desirable as the Cu may come into contact and react with the underlying quartz during oxidation. Furthermore, the Cu_2O will also be bent, strained and difficult to process further. As such the length of the free-standing Cu foils must be limited to less than 30 mm in order to obtain relatively flat Cu_2O.

Recently we showed that in order to obtain high crystal quality and phase purity Cu_2O it is necessary to prevent the thermal oxidation of the Cu during the temperature ramp just prior to the thermal oxidation by using Ar and H_2 as illustrated schematically in Fig. 2(a)–(c).[27] The thermal oxidation of the Cu at 1020 °C occurs at the top and bottom surfaces as shown in Fig. 2(d) and is completed in 30 min as shown schematically in Fig. 2(e). However, the growth of high crystal quality and phase purity Cu_2O is also dependent on the conditions used for cool-down. In the past we removed the Cu_2O crystal rapidly from the heated zone under a flow of Ar after the temperature reached 800 °C similar to Toth *et al.*[19] who obtained Cu_2O from Cu that was subsequently annealed between 1085 °C and 1130 °C for times ranging between 5 and 150 h; the Cu_2O was retracted rapidly in less than 10 s at the end of annealing and the CuO that formed on top of the Cu_2O was removed in HNO_3 (aq) or by the use of abrasives. Others like, Mani *et al.*[25] obtained Cu_2O by thermal oxidation of Cu in air at 1050 °C for 60 min and 1 atm and quenched using a flow of cold Ar at 700 °C.[25]

Here we employed a slow cool down rate to suppress the formation of CuO in Cu_2O as illustrated schematically in Fig. 2(f). More specifically after the completion of thermal oxidation the temperature was reduced from 1020 °C down to 820 °C in a controlled fashion at −5 °C min^{-1} under a flow of 100 ml min^{-1} Ar at 10^{-2} mbar in order to suppress a transition through the CuO/Cu_2O phase-boundary at low and intermediate temperatures which would lead to the precipitation of CuO inside the bulk of the Cu_2O. This is consistent with Chang *et al.*[22] who prepared an ingot of Cu_2O by the optical float zone method that was cut into wafers with a thickness of ∼1 mm and diameters up to 7 mm after which the Cu_2O wafers were annealed in air at 1045 °C for 1 to 4 days at one day intervals. The Cu_2O was removed from the furnace and cooled in air; it reached room temperature in 10 min, but this quenching led to the formation of CuO.[22] It was shown that the density of the Cu vacancies was reduced by slow cooling at −5 °C min^{-1} which also led to a suppression of the formation of CuO on top of the Cu_2O.[21] Similarly, Frazer *et al.*[23] prepared Cu_2O ingots by the floating zone method. Crystal slices of Cu_2O were annealed in a box furnace at 1045 °C for one to five days and cooled to room temperature at a rate of 5 °C min^{-1}. The formation of CuO was suppressed by annealing and slow cooling, which resulted in an increase of phase purity by a factor of 540 ± 70. Consequently, the elimination of O_2 by maintaining a flow of Ar at 10^{-2} mbar during cool down at −5 °C min^{-1} prevents the precipitation of CuO inside the bulk of Cu_2O.

A typical image of the Cu_2O obtained here is shown in Fig. 5(a). The red-ruby Cu_2O observed in transmission is very similar to a naturally occurring red ruby crystal of Cu_2O which

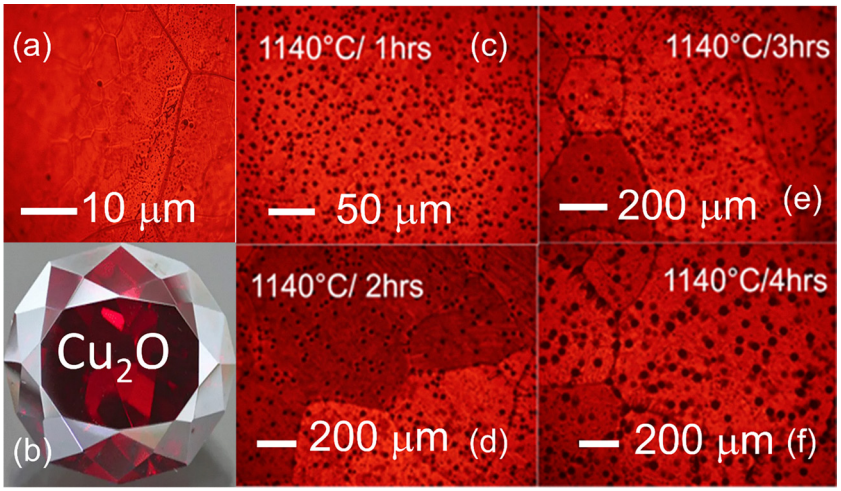

Fig. 5 Typical images of Cu_2O obtained by optical transmission microscopy (a) as grown at 1020 °C (b) natural crystal (c), (d), (e), (f) Cu_2O after annealing at 1140 °C for 1, 2, 3 and h. respectively.

is shown in Fig. 5(b) but a semi-transparent layer of CuO is expected to form on top of the red-ruby Cu_2O. This may be understood as follows: the basic starting point for oxidation of copper to cuprous oxide is $4Cu(s) + 2O_2\ (g) \rightarrow 2Cu_2O(s)$ after which the Cu_2O will be inevitably react with O_2 at the surface according to $2Cu_2O\ (s) + O_2\ (g) \rightarrow 4CuO(s)$ leading to the formation of CuO. The surface layer of CuO is semi-transparent for otherwise we would not be able to see through the Cu_2O crystals of this work under an optical transmission microscope. As such we suggest that the CuO has a thickness of the order of a few tens of nm's similar to what we found previously by TEM/HRTEM.[27]

A typical SEM image of the Cu_2O crystal is shown in Fig. 3(f)–(h). We find that the Cu_2O consists of grains that have sizes up to $\sim 500 \times 500\ \mu m^2$. Interestingly the surface of the Cu_2O is flatter than the Cu after annealing. The Cu_2O exhibited strong peaks in the XRD corresponding to the (111), (110) and (220) crystallographic planes of the cubic crystal structure of Cu_2O. According to Xiao *et al.*[26] strain-driven growth leads to the formation of the (110) and (220) oriented crystallographic planes of Cu_2O but (111) oriented Cu_2O with small grains are obtained by surface energy-dominated growth. It is important to note however that Xiao *et al.*[26] applied strain by constraining the Cu between corundum (Al_2O_3) slides in contrast to the free standing Cu_2O obtained in this work. Despite the fact that we obtain large, single crystal grains of Cu_2O they do not extend all the way through the bulk. The bifacial thermal oxidation of Cu at 1020 °C occurs on the front and back side of the Cu and leads to the formation of a KVL halfway below the surface. A typical SEM image of the KVL is shown on section in Fig. 3(i). We suggest that vacancies and voids are generated at the interface between Cu and Cu_2O due to the large difference in the lattice constants of Cu_2O *i.e.* $a = 4.2696$ Å and that of Cu, $a = 3.615$ Å. The voids grow larger as the two oxidation fronts move into the bulk of Cu. This KVL was originally identified by Toth *et al.*[19] in an indirect way *i.e.* by measuring the resistance along a section but was observed directly by SEM only recently by Xiao *et al.*[26] Consequently, the crystal from top to bottom consists of (i) a compact, semi-transparent thin layer of CuO (ii) single crystal grains of Cu_2O (iii) a layer of Kirkendall voids (iv) single crystal grains of Cu_2O and finally (v) a CuO layer on the back as depicted schematically in Fig. 3(f). Obviously the KVL and the semi-transparent surface layer of CuO must be eliminated.

We have tried to remove the KVL by annealing the Cu_2O at 1120 °C, 1140 °C and 1160 °C for 60 min; SEM images on plan and section are shown in Fig. 6(A) to (C) respectively. We also annealed the Cu_2O at 1140 °C under Ar for 2, 3 and 4 hours; plan view images are shown in Fig. 7(A) to (C) respectively. One may observe the formation of well defined, steps and holes in Fig. 6(A) after annealing the Cu_2O at 1120 °C for 60 min; the formation of the holes at the surface is attributed to the out-diffusion of copper vacancies and Kirkendall voids during recrystallization so that the energy of the crystal is minimized. The circular holes after annealing at 1120 °C are empty and have a diameter of ~ 1 μm. We find that the areal density of the holes exhibits a strong increase after annealing at 1140 °C as shown in Fig. 6(B). The holes appear as black dots in optical transmission. Interestingly we observe that most of the holes are filled up with individual lamellas that are oriented in various directions and protrude above the surface as shown in Fig. 6(B) and the Kirkendall voids do not form an extended layer as shown in Fig. 3(i). The Kirkendall voids are nearly eliminated after annealing at 1160 °C as shown in Fig. 6(C) but the diameter of the holes has increased up to ~ 10 μm. We estimate that the diffusion coefficient is of the order of 10^{-10} at 1160 °C which is quite high, taking a vacancy migration activation energy of ~ 1.0 eV and $D_0 \sim 10^{-6}\ m^2\ s^{-1}$. In short, the KVL can be reduced significantly by annealing above 1200 °C but this inevitably leads to the formation of holes in the vicinity of the surface.

In addition to varying the temperature of annealing we also varied the time of annealing. Typical SEM images of the Cu_2O annealed at 1140 °C for 2, 3 and 4 h. are shown in Fig. 7(A) to (C) respectively. One may again observe the formation of holes

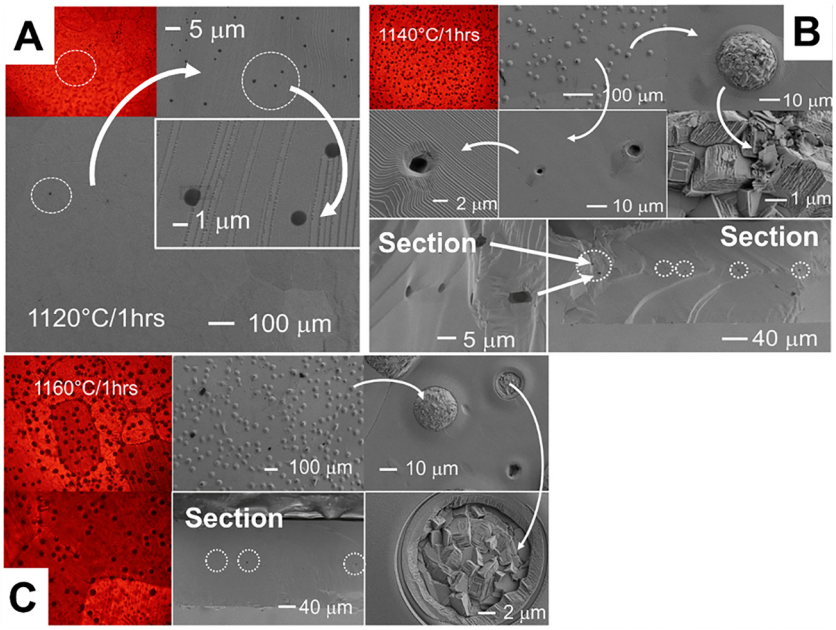

Fig. 6 SEM images of Cu_2O annealed at 1120 °C, 1140 °C and 1160 °C for 1 h under a flow of Ar shown in panels A, B and C respectively; also shown for completeness corresponding images of Cu_2O obtained by optical transmission microscopy showing the red-ruby Cu_2O. (a) Empty pinholes and steps appear on the surface after annealing at 1120 °C for 1 h. (b) The density of the pinholes is larger after annealing at 1140 °C for 1 h; some of the pinholes are filled with crystals having a lamella crystal structure and some are empty; also shown the KVL on section showing voids that have a size of ~5 μm (c) Similar pinholes are observed after annealing at 1160 °C for 1 h; the KVL has been nearly eliminated as shown on section.

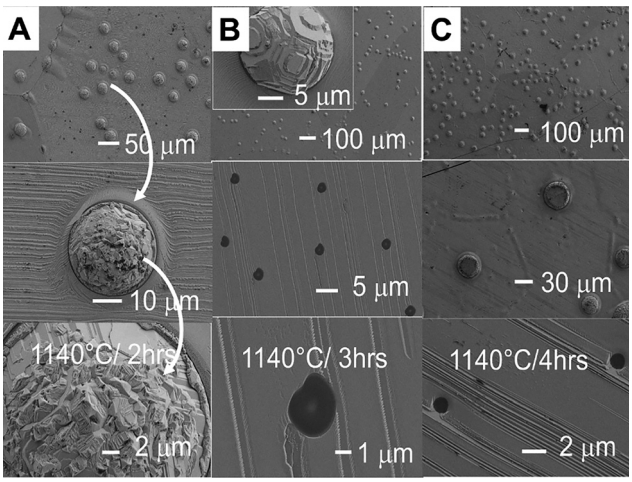

Fig. 7 SEM images of Cu_2O annealed at 1140 °C for 2, 3 and 4 h under a flow of Ar at 1 atm shown in panels A, B and C respectively; different magnifications are shown top to bottom as indicated by the arrows in each case. One may observe the occurrence of partially and completely filled pinholes as well as steps on the surface in all three cases.

on the surface of the Cu_2O crystal, some of which are hollow, and others filled with individual lamellas that are oriented in various directions and protrude above the surface as shown in Fig. 7(A). The recrystallization of these lamellas occurs with increasing time and ordered facets develop as shown in Fig. 7(B) and (C) after annealing at 1140 °C for 3 and 4 h respectively. In addition, one may observe the filling of the empty holes. In all cases recrystallization has led to the formation of steps on the surface. Before elaborating further, it is interesting to point out that these spherical protrusions extend downwards into the bulk Cu_2O up to 30 μm as shown by the SEM section images of the Cu_2O after annealing at 1040 °C up to 4 h in Fig. 8(A) and (B). All of the Cu_2O crystals annealed between 1120 and 1160 °C for 1 h exhibited clear peaks in the XRD as shown in Fig. 4(b); one may observe only peaks corresponding to the (110), (220) and (111) crystallographic orientations of Cu_2O annealed at 1120 °C for 1 h and the emergence of peaks corresponding to the (111), (200) and (220) crystallographic orientations of Cu upon annealing at 1140 °C and 1160 °C for 1 h. The high temperature annealing was carried out under inert Ar to prevent the reaction of the Cu_2O with O_2 which would lead to the formation of CuO. The use of Ar translates into a lack of oxygen, so the Cu_2O is losing oxygen and Cu is precipitating into the voids above its melting point *i.e.* 1085 °C that's why we observe semi-spherical protrusions on the surface and peaks corresponding to Cu in the XRD. Similar trends are observed after annealing the Cu_2O at 1140 °C for 2, 3 and 4 h. Moreover, we find that the Cu_2O is compressively strained, and the strain is ~0.94% before annealing but is reduced to ~0.46% after annealing. The strain in the Cu_2O during thermal oxidation of Cu occurs due to the difference in the lattice constants as well as thermal expansion coefficients of Cu and Cu_2O.

From the above it is evident that the KVL must be removed by polishing not by annealing in order to preserve the single crystal nature of the Cu_2O grains. This may be achieved by polishing the Cu_2O crystal from the back side. However, the Cu_2O crystal is brittle and not easy to cleave in straight lines due to the fact that it consists of interlocked polygon grains. In

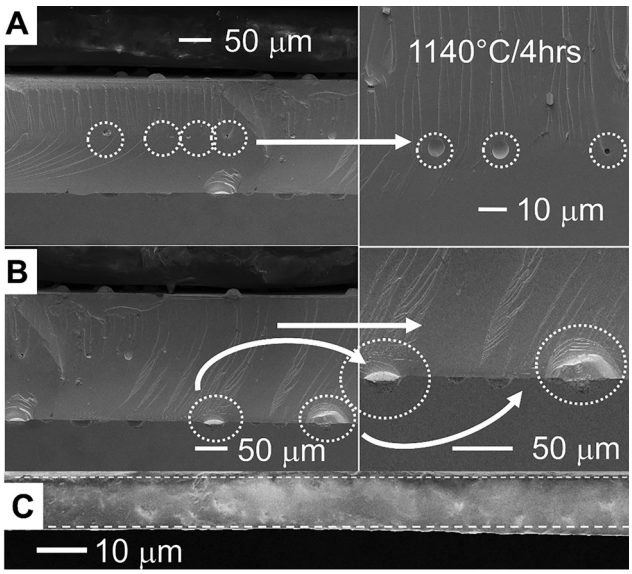

Fig. 8 SEM images of Cu_2O on section after annealing at 1140 °C for 4 h. (A) A reduction in the extent of the KVL layer and isolated spherical voids are observed (B) section showing filled up holes below and above the surface (C) a section of the polished Cu_2O obtained at 1120 °C with no post growth annealing.

addition, the Cu_2O crystal is not perfectly flat. In general, the Cu_2O crystals obtained *via* the thermal oxidation of free-standing Cu with a length to width ratio >2 exhibited bowing and were bent along the lateral direction. The Cu_2O crystals obtained from Cu with $l/w = 1$ were bent along all sides.

In order to obtain a relatively flat piece of crystal from the Cu_2O we had to remove the corner supports and then apply pressure between two glass slides. The Cu_2O broke into irregular pieces similar to the natural red-ruby Cu_2O crystal fragments that were used by Kazimierczuk *et al.*[6] for the observation of giant Rydberg excitons as well as Orfanakis *et al.*[7] who integrated them into a $SiO_2/Ta_2O_5/Cu_2O/Ta_2O_5/SiO_2$ Fabry–Pérot cavity. The natural Cu_2O crystals in both of these cases had dimensions of ~ 3 mm $\times$ 3 mm.[6,7] The Cu_2O pieces that we obtained have similar dimensions of ~ 5 mm $\times$ 5 mm. A section of the Cu_2O after polishing is depicted in Fig. 8(C) showing that the KVL has been removed successfully without annealing.

Finally, the semi-transparent layer of CuO at the surface also has to be removed by polishing. CuO is a p-type metal-oxide semiconductor that has an indirect energy gap of 1.4 eV and will absorb photons bouncing back and forth between the mirrors of a cavity. The CuO will absorb photons and also act as a sink for the photogenerated electron and holes which will recombine in a non-radiative fashion in the near vicinity of the surface especially *via* deep states in the energy gaps of the CuO and Cu_2O that are related to crystallographic imperfections that form due to the difference in their lattice constants. Nevertheless, it is important to keep in mind that this layer of CuO acts as an excellent passivation layer for the underlying red ruby Cu_2O so it can be stored for extended periods of time under ambient conditions.

Considering that the Cu_2O crystals are very brittle especially after removing the KVL by polishing down to a few tens of μm, it is difficult to use them as substrates for the subsequent deposition of other n-type oxides *e.g.* ZnO and processing to make p–n junction solar cell devices. One way of overcoming these difficulties is to bond them onto a rigid substrate after removing the voids which would allow subsequent processing to be carried out, but the Cu_2O would have to be doped during growth with a suitable p-type impurity in order to increase its conductivity and reduce resistance as the Cu_2O crystals in our case did not contain any intentional p-type impurities. Nevertheless, we must point out that the free standing Cu_2O crystals obtained using the method described here is not cost effective or justified for the fabrication of competitive solar cell devices. Lower cost methods such as reactive sputtering of Cu_2O are more suitable as described by Shibasaki *et al.*[3] who fabricated an all-oxide solar cell with an efficiency of $\sim 10\%$.

4. Conclusions

Cu_2O has been obtained *via* the thermal oxidation of Cu under Ar and O_2 at 1020 °C followed by controlled cooldown at -5 °C at 10^{-2} mbar under an inert flow of Ar. We obtain single crystal grains of Cu_2O with sizes of $\sim 500 \times 500$ μm^2 which have a cubic crystal structure and extend down to a layer of Kirkendall voids that form in the middle due to the bifacial oxidation of the Cu in ~ 6 hours without annealing the Cu_2O. Annealing between 1120 °C and 1160 °C leads to a significant reduction of the Kirkendall voids and grain growth up to 3×3 mm^2 but also the formation of 10–20 μm deep holes due to the extensive out diffusion of the Kirkendall voids that are gradually filled with Cu upon increasing the annealing temperature due to a transition through the Cu_2O/Cu phase boundary. The growth of the free standing Cu_2O carried out in this way uses a high thermal budget but one may isolate individual Cu_2O grains after removing the KVL by polishing for the purpose of optical spectroscopy without the need for extensive, long annealing, thereby minimizing as much as possible the thermal budget. The Cu_2O crystals obtained in this way are not cost effective for the fabrication of competitive, all-oxide, solar cell devices for which lower cost methods such as reactive sputtering are more suitable.

Author contributions

Matthew Zervos, G. Georgiadis, were responsible for the growth and annealing of the Cu_2O, x-ray diffraction, optical transmission microscopy and writing up; Ioannis Paschos, Matin Ashurov and Pavlos Savvidis were responsible for scanning electron microscopy, atomic force microscopy, polishing and writing up.

Conflicts of interest

There are no conflicts of interest to declare.

Data availability

All data supporting this article has been included in the mani manuscript.

Acknowledgements

The authors acknowledge funding from the Innovation Program for Quantum Science and Technology (2023ZD0300300) and the Innovation Resource Allocation of Westlake University-Zhejiang Provincial Natural Science Foundation of China under Grant No. XHD24A2401

References

1 E. F. Gross, Optical Spectrum of Excitons in the Crystal Lattice, *Nuovo Cimento*, 1956, **3**, 672–701.
2 C. Malerba, F. Biccari, C. L. A. Ricardo, M. D'Incau and P. Scardi, A. Mittiga, Absorption Coefficient of Bulk and Thin Film Cu_2O, *Sol. Energy Mater. Sol. Cells*, 2011, **95**, 2848–2854.
3 S. Shibasaki, Y. Honishi, N. Nakagawa, M. Yamazaki, Y. Mizuno, Y. Nishida, K. Sugimoto and K. Yamamoto, Highly Transparent Cu_2O Absorbing Layer for Thin Film Solar Cells, *Appl. Phys. Lett.*, 2021, **119**, 242102.
4 Y. H. Zhang, M. M. Liu, J. L. Chen, S. M. Fang and P. P. Zhou, Recent Advances in Cu_2O-Based Composites for Photocatalysis: A Review, *Dalton Trans.*, 2021, **50**, 4091–4111.
5 G. Liu, F. Zheng, J. Li, G. Zeng, Y. Ye, D. M. Larson, J. Yano, E. J. Crumlin, J. W. Ager, L. Wang and F. M. Toma, Investigation and Mitigation of Degradation Mechanisms in Cu_2O Photoelectrodes for CO_2 Reduction to Ethylene, *Nat. Energy*, 2021, **6**, 1124–1132.
6 T. Kazimierczuk, D. Fröhlich, S. Scheel, H. Stolz and M. Bayer, Giant Rydberg excitons in the Copper Oxide Cu_2O, *Nature*, 2014, **514**, 343–347.
7 K. Orfanakis, S. K. Rajendran, V. Walther, T. Volz, T. Pohl and H. Ohadi, Rydberg Exciton–Polaritons in a Cu_2O Microcavity, *Nat. Mater.*, 2022, **21**, 767–772.
8 K. Kawaguchi, R. Kita, M. Nishiyama and T. Morishita, Molecular Beam Epitaxy Growth of CuO and Cu_2O Films with Controlling the Oxygen Content by the Flux Ratio of Cu/O, *J. Cryst. Grow.*, 1994, **143**, 221–226.
9 T. Iivonen, M. J. Heikkilä, G. Popov, H. E. Nieminen, M. Kaipio, M. Kemell, M. Mattinen, K. Meinander, K. Mizohata, J. Räisänen, M. Ritala and M. Leskelä, Atomic Layer Deposition of Photoconductive Cu_2O Thin Films, *ACS Omega*, 2019, **4**, 11205–11214.
10 S. F. U. Farid, D. Cherns, J. A. Smith, N. A. Fox and D. J. Fermín, Pulsed Laser Deposition of Single-Phase n- and p-type Cu_2O Thin Films with Low Resistivity, *Mater. Design*, 2020, **193**, 108848.
11 A. S. Rahman, M. A. Islam and K. M. Shorowordi, Electrodeposition and Characterization of Copper Oxide Thin Films for Solar Cell Applications, *Procedia Eng.*, 2015, **105**, 679–685.
12 H. Liu, V. H. Nguyen, H. Roussel, I. Gélard, L. Rapenne, J. L. Deschanvres, C. Jiménez and D. Muñoz-Rojas, The Role of Humidity in Tuning the Texture and Electrical Properties of Cu_2O Thin Films Deposited *via* Aerosol-Assisted CVD, *Adv. Mater. Interfaces*, 2018, **6**, 1801364.
13 S. Chatterjee and A. J. Pal, Introducing Cu_2O Thin Films as a Hole-Transport Layer in Efficient Planar Perovskite Solar Cell Structures, *J. Phys. Chem. C*, 2016, **120**, 1428–1437.
14 S. Steinhauer, M. A. M. Versteegh, S. Gyger, A. W. Elshaari, B. Kunert, A. Misiewicz and V. Zwiller, Rydberg Excitons in Cu_2O Microcrystals Grown on a Silicon Platform, Nature Communication, *Materials*, 2020, 1–11.
15 G. Blankenbur and K. Kassel, Fehlordnung und Elektrisches Verhalten der Ionenund Valenzkristalle, *Ann. Phys.*, 1952, **10**, 201–216.
16 J. H. Apfel and L. N. Hadley, Exciton Absorption in Cuprous Oxide, *Phys. Rev.*, 1955, **100**, 1689–1691.
17 K. Stecker, Über die Halbleitereigenschaften des Kupferoxyduls. XII Die Leitfähigkeit des Kupferoxyduls innerhalb des Existenzgebietes bei hohen Temperaturen im Bereich kleiner Drucke, *Ann. Phys.*, 1959, **458**, 55–69.
18 R. Frerichs and R. Handy, Electroluminescence in Cuprous Oxide, *Phys. Rev.*, 1959, **113**, 1191–1198.
19 R. S. Toth, R. Kilkson and D. Trivich, Preparation of Large Area Single-Crystal Cuprous Oxide, *J. Appl. Phys.*, 1960, **31**, 1117–1121.
20 W. S. BrowerJr and H. S. Parker, Growth of Single Crystal Cuprous Oxide, *J. Cryst. Grow.*, 1971, **8**, 227–229.
21 R. D. Schmidt-Whitley, M. Martinez-Clemente and A. Revcolevschi, Growth and Microstructural Control of Single Crystal Cuprous Oxide Cu_2O, *J. Cryst. Grow.*, 1974, **23**, 113–120.
22 K. B. Chang, L. Frazer, J. J. Schwartz, J. B. Ketterson and K. R. Poeppelmeier, Removal of Copper Vacancies in Cuprous Oxide Single Crystals Grown by the Floating Zone Method, *Cryst. Growth Des.*, 2013, **13**, 4914–4922.
23 L. Frazer, K. B. Chang, K. R. Poeppelmeier and J. B. Ketterson, Cupric Oxide Inclusions in Cuprous Oxide Crystals Grown by the Floating Zone Method, *Sci. Technol. Adv. Mater.*, 2015, **16**, 034901.
24 S. A. Lynch, C. Hodges, S. Mandal, W. Langbein, R. P. Singh, L. A. P. Gallagher, J. D. Pritchett, D. Pizzey, J. P. Rogers, C. S. Adams and M. P. A. Jones, Rydberg Excitons in Synthetic Cuprous Oxide (Cu_2O), *Phys. Rev. Mater.*, 2021, **5**, 084602.
25 S. Mani, J. I. Jang, J. B. Ketterson and H. Y. Park, High-Quality Cu_2O crystals with Various Morphologies Grown by Thermal Oxidation, *J. Cryst. Grow.*, 2009, **311**, 3549–3552.
26 M. Xiao, P. Gui, K. Dong, L. Xiong, J. Liang, F. Yao, W. Li, Y. Liu, J. Li, W. Ke, C. Tao and G. Fang, Quasi-Single Crystalline Cuprous Oxide Wafers *via* Stress-Assisted Thermal Oxidation for Optoelectronic Devices, *Adv. Funct. Mater.*, 2022, **32**, 2110505.
27 M. Zervos, I. Paschos, P. Savvidis, N. Florini, K. Koutsokostas, P. Komninou and N. Lathiotakis, *Cryst. Eng. Commun.*, 2025, **27**, 1977–1985.
28 K. Y. Maimaiti, M. Nolan and S. D. Elliott, Reduction Mechanisms of the CuO(111) Surface Through Surface Oxygen Vacancy Formation and Hydrogen Adsorption, *Phys. Chem. Chem. Phys.*, 2014, **16**, 3036–3046.
29 S. Jin, M. Huang, Y. Kwon, L. Zhang, B. W. Li, S. Oh, J. Dong, D. Luo, M. Biswal, B. V. Cunning, P. Bakharev, I. Moon, W. J. Yoo, D. C. Camacho-Mojica, Y. J. Kim, S. H. Lee, B. Wang, W. K. Seong, M. Saxena, F. Ding, H. J. Shin and R. Ruoff, Colossal Grain Growth Yields Single-Crystal Metal Foils by Contact-Free Annealing, *Science*, 2018, **362**, 1021–1025.